Supporting Information for

‘Homogeneous Large-Area Quasi-Free-Standing Monolayer and Bilayer Graphene on SiC’

D. Momeni Pakdehi,[,†] K. Pierz,[*,†] S. Wundrack,[†] J. Aprojanz,[‡] T. T. N. Nguyen,[§] T. Dziomba,[†] F. Hohls,[†] A. Bakin,[⊥,∥] R. Stosch,[†] C. Tegenkamp,[§,‡], F. J. Ahlers,[†] and H. W. Schumacher[†]*

[†]Physikalisch−Technische Bundesanstalt, Bundesallee 100, 38116 Braunschweig, Germany

[‡]Institut für Festkörperphysik, Leibniz Universität Hannover, Appelstraße 2, 30167 Hannover, Germany

[§]Institute of Physics of Technische Universität Chemnitz, Reichenhainer Straße 70, 09126 Chemnitz, Germany

[⊥]Institut für Halbleitertechnik, Technische Universität Braunschweig, Hans−Sommer Straße 66, 38106 Braunschweig, Germany

[∥]Laboratory of Emerging Nanometrology (LENA), Technische Universität Braunschweig, Langer Kamp 6a, 38106 Braunschweig, Germany

*E-mail: davood.momeni.pakdehi@ptb.de.

*E-mail: klaus.pierz@ptb.de.

Influence of Argon Flow Rate on Conventional Epitaxial Sublimation Growth (SG) of Buffer Layer

Figure S1 shows the influence of the argon mass flow rate on buffer layer growth on the samples without polymer preparation which are investigated by AFM and SEM. Three samples S'_0, S'_{100}, and S'_{1000} are 4H−SiC with nominal miscut of about −0.06° toward $[1\bar{1}00]$ and were processed at 1400 °C (1 bar argon atmosphere, for 30 min) at different Ar flow of 0, 100 and 1000 sccm, respectively. This experiment was carried out under the same conditions as the one in the manuscript and it aims at studying the influence of argon flow on samples grown from another SiC polytype (4H−SiC) in the absence of polymer preparation. For the high argon flow of 1000 sccm, the surface of the sample undergoes severe step bunching without any buffer layer growth Figure S1g−i. This is similar to the PASG sample in the manuscript (see Figure 2g−i). In both cases, the high Ar flow leads to surface etching. For moderate Ar flow, however, the situation is different. The surface of the sample without polymer preparation shows stripes of the covered buffer layer and bare SiC, Figure S1d−f. This is in contrast to the PASG sample (manuscript Figure 2d−f) where the provided carbon species from the polymer lead to surface super−saturation and well buffer layer coverage although there the Ar flow caused canyonlike defects. For the case of zero argon flow (Figure S1a−c) the surface looks very good with homogeneous coverage, while the terraces appear less ordered in comparison with the PASG sample (manuscript Figure 2a−c).

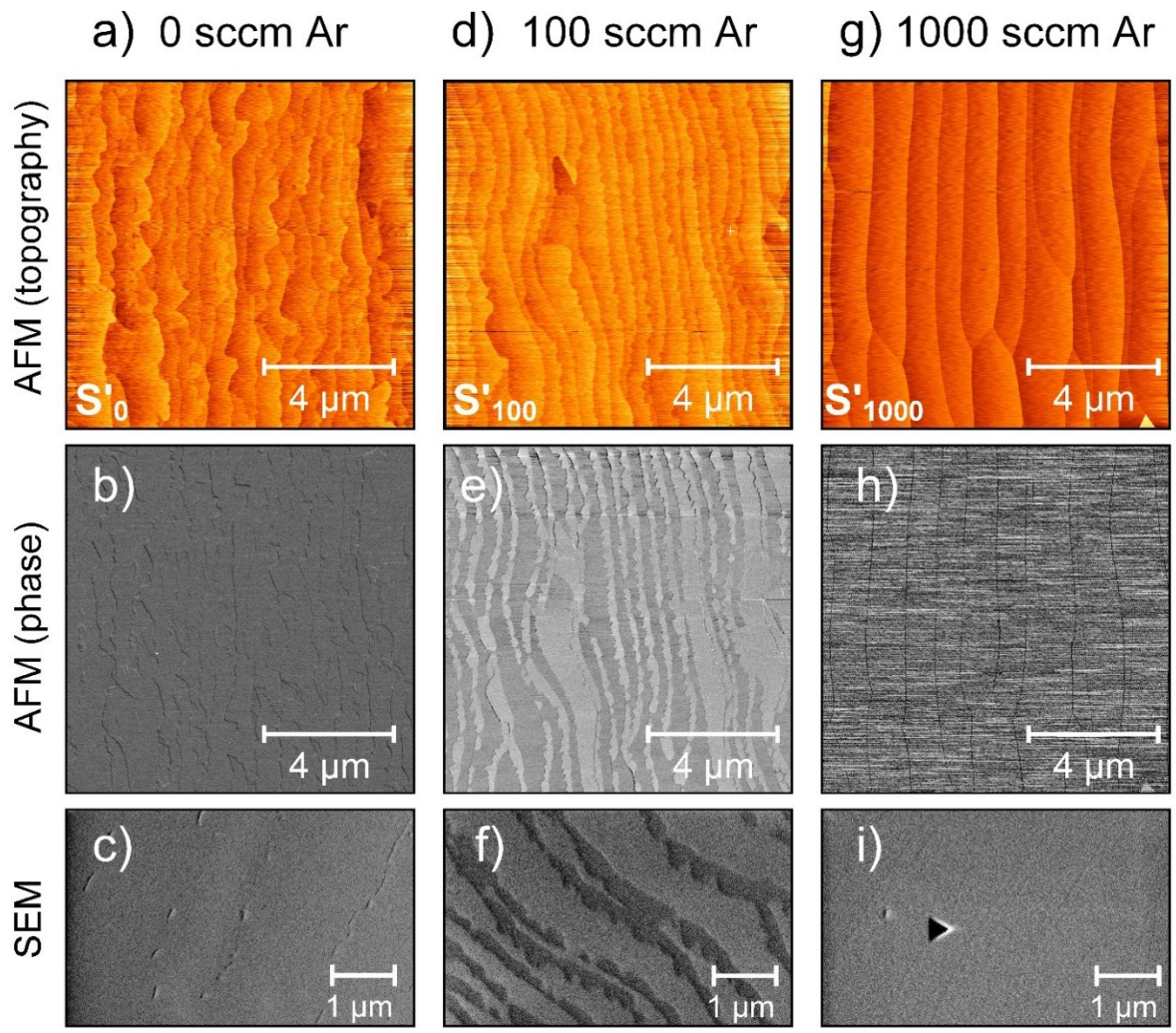

Figure S1. Inspection of the influence of the argon mass flow rate on graphitization of 4H−SiC(0001) at 1400°C (1bar Ar ambient, 30 min) under three different argon gas flows: a) S'_0 (Ar/ 0 sccm), b) S'_{100} (Ar/100 sccm), and c) S'_{1000} (Ar/1000 sccm). The sample was grown by conventional sublimation growth without polymer preparation. S'_0 processed under no Ar flow representing good buffer layer coverage in AFM phase (b) and scanning electron microscopy SEM (1kV) (c) images. The moderate flow Ar for S'_{100} distorts its surface growth causing the formation of the buffer layer stripes on this sample, as can be seen in AFM phase (e) and SEM (f) images. The intensive argon flux on S'_{1000} prevents buffer layer formation and results in severe step bunching on this sample (g), (h), (i).

Formation of Triangular-Shape Structures

We observed that the increase of the Ar flow leads to a formation of a triangular-shape structures. This can be seen in Figure S1g−i, for the sample processed under 1000 sccm Ar flow. Also, further increase of the Ar flow escalates the density of such structures, as can be seen in Figure S2, for the sample processed at 1400 °C (30 min, 1 bar Ar) in the presence of the Ar flow rate of 2000 sccm. The aggregated mass along the giant steps and the triangular-like structures is a typical morphology all over the surface of this sample. Although, here the properties of such triangular-shape structures has not been further studied, however, they very resemble the cubic SiC grown on other substrates elsewhere.[1,2]

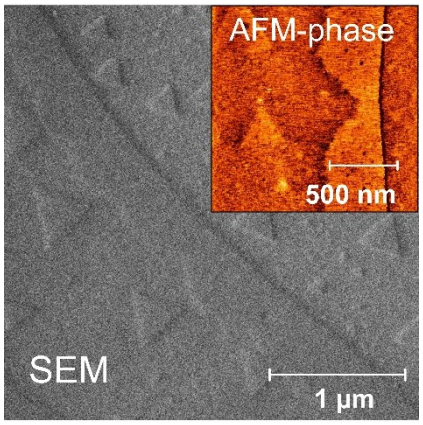

Figure S2. Formation of triangular-like structures at high argon gas flow. Scanning electron micrograph (1kV) of a 6H−SiC sample after annealing at 1400°C (1 bar in Ar ambient, 30 min) under 2000 sccm Ar flow rate. The inset shows the AFM phase image of the same sample.

Moreover, such triangular-shape structures could also appear under a lower growth pressure, in which leads to condensation and reflection of sublimated species back onto the surface of the substrate. Figure S3 shows AFM inspection on the surface of a 6H−SiC sample which processed at 50 mbar in argon ambient (1400 °C, 30 min). The triangular-shape structures appear to cover entire the substrate with heights up to 14 nm.

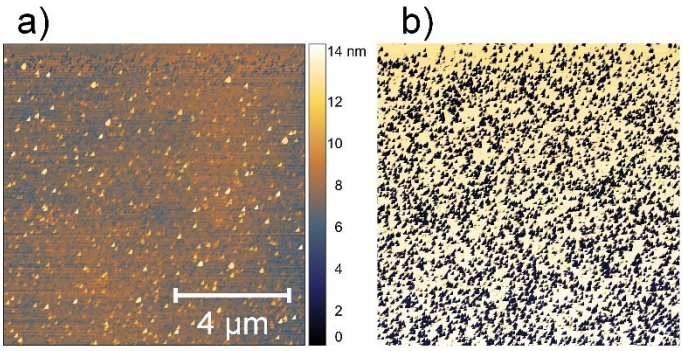

Figure S3. AFM inspection: (a) morphology (b) phase image. Triangular-shape structures appeared on the surface of a sample processed at 1400 °C (30 min), but the pressure was 50 mbar instead of the typical 1 bar of argon. The surface shows high condensation of the sublimated species back on the surface of the sample.

Step-by-Step Transition of Buffer Layer to Quasi-Free-Standing Monolayer Graphene

Figure S4a shows the Raman spectra of a buffer layer sample after step−by−step hydrogen intercalation 5% (95% argon) for 15 minutes at different temperatures ranging from 400 °C up to 1200 °C. The intercalation up to 400 °C does not show any significant change in the buffer layer spectra with the typical two−phonon bands in the spectral range between 1390 and 1605 cm^{-1}. [3] By temperature rise to 500°C despite the slight change in D−peak, yet no 2D−peak is observed, whereas at 600°C the D−peak sharply increases and the 2D−peak is observed, clearly indicating a transition from the buffer layer to graphene. By further increasing temperature, the D−peak decreases, which denotes disorder reduction in the crystal of graphene. An even higher temperate leads to a higher 2D−peak, while its position shifts to lower wave numbers. This is the result of a tensile strain which may be accompanied with a doping increase.[4,5] Moreover, the increase of the temperature shows lowering down the defect density of the QFMLG layer as shown for three annealing steps of 600 °C, 800 °C, and 1000 °C, in Figure S4b−d. We also observed a similar transition of the buffer layer to QFMLG via intercalation of ultralow concentration of oxygen in nitrogen atmosphere.[6]

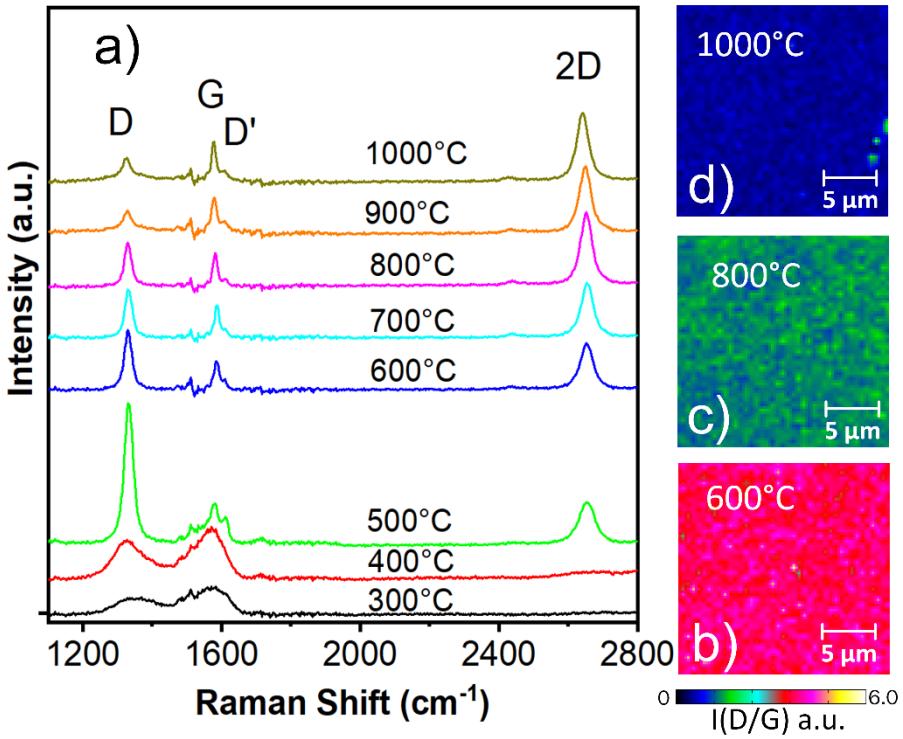

Figure S4. Temperature dependency of intercalation on buffer layer sample via 5% (95%Ar) hydrogen. At 400 °C, no intercalation occurred, inferred from the Raman spectra (a). For temperature above 400°C, the D−peak starts to increase which is accompanied by the appearance of 2D−peak at 600°C, indicating a transition to graphene. By increasing the temperature, D−peak decreases and 2D−peak increases demonstrating more effective intercalation and reduction of defect density measured by I_D/I_G (b−d).

Hydrogen Intercalation on Low−Quality Buffer Layer:

Figure S5 shows the AFM and Raman investigations of a buffer layer sample with poor coverage. The AFM phase images (Figure S5b) shows a color contrast on the abutting terraces, although the origin of the contrast is different from the optimized sample in the manuscript (see Figure 4b). The contrast on this sample is a result of interaction between AFM tip with two different materials (buffer layer and SiC stripes) directly at the sample surface (see the profile in Figure S5e), whereas the contrast on the optimized sample is attributed to the underlying SiC surfaces. The Raman mapping of D+G areas in Figure S5d shows an inhomogeneous buffer

layer. Accordingly, as it was expected, the hydrogen intercalation on such defected buffer layer has led to a highly defected QFMLG, as shown in the Raman mapping of I_D/I_G in Figure S5f.

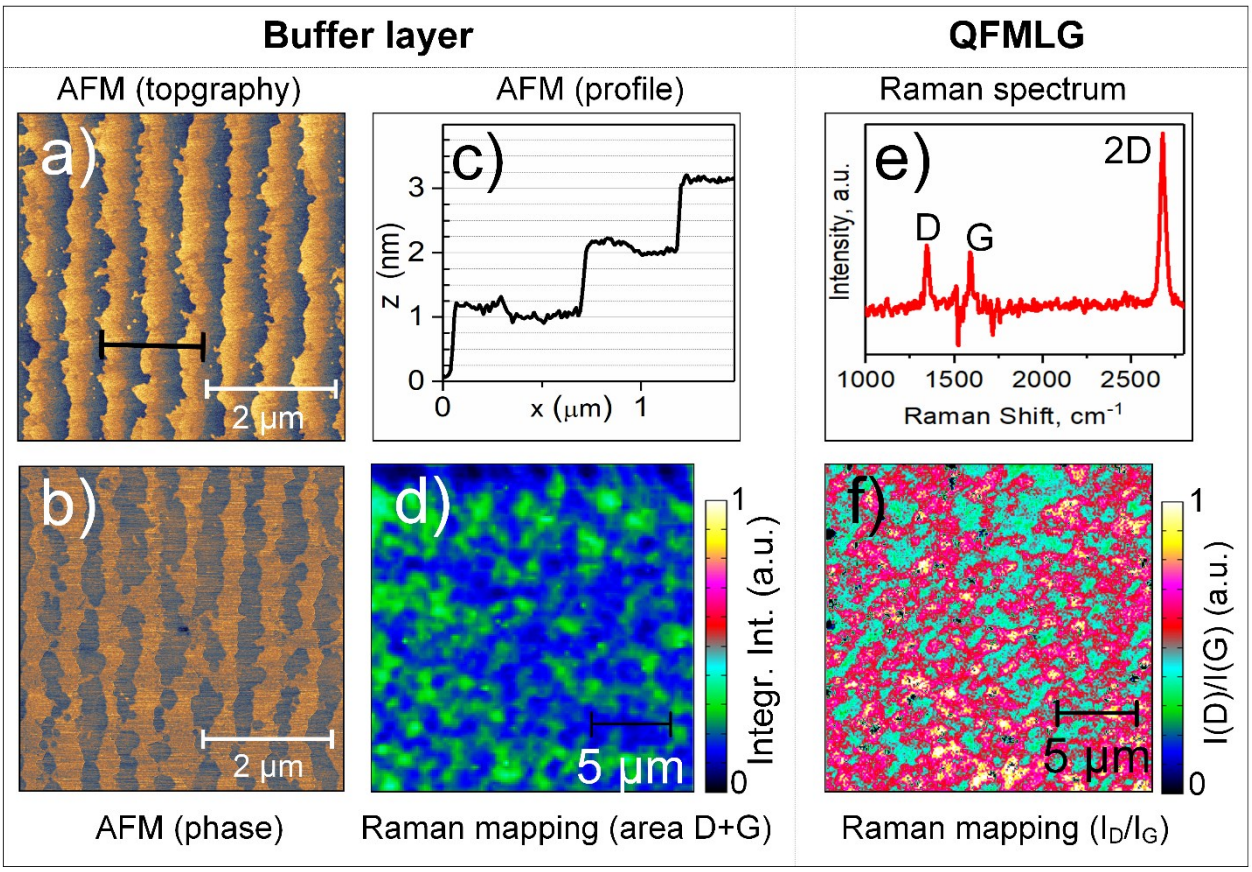

Figure S5. AFM topography (a), height profile (b) and phase (c) images of a buffer layer sample with poor coverage showing a phase color contrast corresponding to SiC and buffer layer stripes. (d) Raman mapping of D+G peaks area of the buffer layer. (e) Raman spectrum of the sample after the intercalation by hydrogen 5% (95% Ar). f) Raman Mapping of *I* (D/G) shows an inhomogeneous QFMLG.

Atomic Resolution STM Measurement on QFMLG.

Figure S6a shows a two−dimensional STM image captured on QFMLG sample shown in the manuscript (see Figure 4d) with a larger size of 15 x 15 nm^2. It can be seen that the quasi-free-standing monolayer graphene passes very smoothly over the step of 0.25 nm high from one terrace to the adjacent terrace. Figure S6b exhibits the QFMLG nicely covers a higher step of 0.75 nm high (1/2 unit−cell of 6H−SiC) which randomly was observed on this sample.

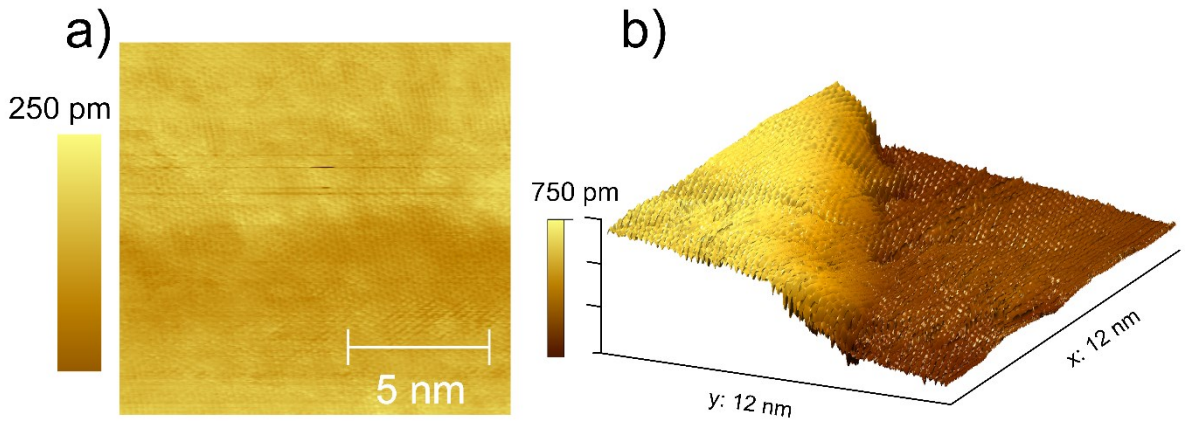

Figure S6. STM topography inspection of QFMLG (shown in the manuscript in Figure 4) on (a) a terrace with the step of 0.25 nm high and (b) a terrace with the step height of 0.75 nm.

Raman 2D−Peak Spectrum of Quasi-Free-Standing Bilayer Graphene

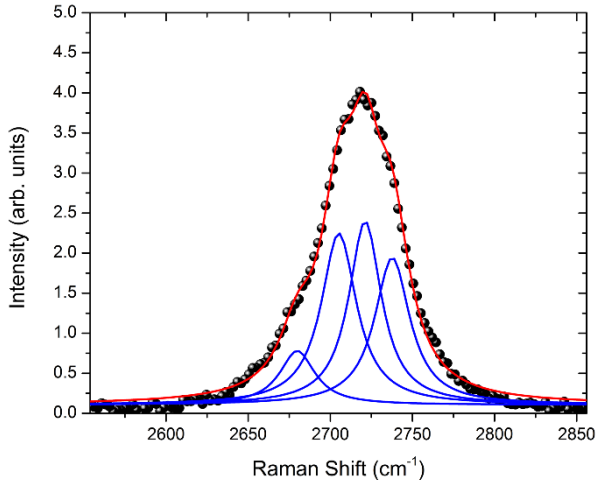

Figure S7. Raman spectrum of QFBLG shows broadened 2D−peak with an FWHM of ~ 59 cm^{-1} as well as an asymmetrical line shape of the 2D−peak which can be fitted by four Lorentzian curves.

REFERENCES

(1) Frewin, C. L.; Locke, C.; Wang, J.; Spagnol, P.; Saddow, S. E. *J. Cryst. Growth* **2009**, *311* (17), 4179–4182.

(2) Suemitsu, M.; Jiao, S.; Fukidome, H.; Tateno, Y.; Makabe, I.; Nakabayashi, T. *J. Phys. D. Appl. Phys.* **2014**, *47* (9).

(3) Fromm, F.; Oliveira, M. H.; Molina-Sánchez, A.; Hundhausen, M.; Lopes, J. M. J.; Riechert, H.; Wirtz, L.; Seyller, T. *New J. Phys.* **2013**, *15* (0001), 1–12.

(4) Fromm, F.; Wehrfritz, P.; Hundhausen, M.; Seyller, T. *New J. Phys.* **2013**, *15* (0001).

(5) Das, A.; Pisana, S.; Chakraborty, B.; Piscanec, S.; Saha, S. K.; Waghmare, U. V.; Novoselov, K. S.; Krishnamurthy, H. R.; Geim, A. K.; Ferrari, A. C.; Sood, A. K. *Nat. Nanotechnol.* **2008**, *3* (4), 210–215.

(6) Wundrack, S.; Momeni Pakdehi, D.; Schädlich, P.; Speck, F.; Pierz, K.; Seyller, T.; Schumacher, H. W.; Bakin, A.; Stosch, R. *Phys. Rev. B* **2019**, *99* (4), 045443.